Cyanidin-3-O-glucoside enhances GLP-1 secretion via PPARβ/δ-β-catenin-TCF-4 pathway in type 2 diabetes mellitus

Check for updates

Xiang Ye[1,2,3], Wen Chen[3], Fujie Yan[3], Xiaodong Zheng[3] & Pengcheng Tu[1] ✉

In late-stage type 2 diabetes mellitus (T2DM), impaired islet β cell function leads to absolute insulin deficiency, thereby disrupting blood glucose homeostasis. GLP-1, an incretin hormone, stimulates insulin secretion from islet β cells post-meals. This study investigated the effects of anthocyanin cyanidin-3-O-glucoside (C3G) on GLP-1 secretion using STC-1 (intestinal endocrine L cells) and NIT-1 (islet β cells). In a co-culture system, C3G treatment increased GLP-1 secretion in STC-1 cells, promoting insulin release in NIT-1 cells under high glucose. Mechanistically, C3G activated the PPARβ/δ-β-catenin-TCF-4 pathway in STC-1 cells, enhancing PG precursor transcription and GLP-1 synthesis.Inhibiting PPARβ/δ with GSK0660 blocked this C3G-induced upregulation. Overall, C3G stimulates GLP-1 secretion from intestinal L cells via this pathway, indirectly boosting insulin release from β cells. These findings enhance T2DM mechanism understanding and suggest the potential of C3G in GLP-1-based T2DM therapy.

The global burden of diabetes continues to escalate, impacting individuals, families, and countries significantly. Notably, over 90% of those affected with type 2 diabetes mellitus (T2DM)[1]. In the early stages of T2DM, insulin demand increases due to peripheral insulin resistance, when the body compensates by stimulating islet β cells to release more insulin, thereby maintaining blood glucose stability. However, in the later stages, impaired islet β cell function due to prolonged hyperglycemia causes the absolute deficiency of insulin in the body[2], and insulin remains the first-line treatment for T2DM. Therefore, finding appropriate methods to regulate insulin levels in the body may provide new and effective means for the treatment of T2DM.

Encoded by the proglucagon (PG) gene, glucagon-like peptide-1 (GLP-1)[3], which is secreted by intestinal L cells during the postprandial state, has been confirmed to play a significant role in glucose metabolism in multiple human and animal studies. Researchers have found that disruption of the GLP-1 receptor gene can lead to abnormal glucose tolerance in mice[4]. Compared to healthy individuals, GLP-1 treatment would increase the insulin level stimulated by diet and inhibit postprandial hyperglycemia without causing hypoglycemia[5]. Currently, clinical treatment mainly relies on oral DPP-4 inhibitors to maintain GLP-1 levels. However, another approach could be to increase endogenous GLP-1 production by regulating the transcription of the PG gene in intestinal endocrine L cells[6].

The PG promoter contains several transcriptional control elements, among which the G2 response element is closely related to tissue-specific regulation of PG transcription[7]. Research has found that insulin inhibitors can stimulate the activity of the G2 response element in intestinal endocrine L cells through the β-catenin/TCF-4 signaling pathway, thereby increasing GLP-1 production[8].

The transcription factor peroxisome proliferator-activated receptor (PPAR), which includes three isoforms: PPARα, PPARγ, and PPARβ/δ, has been reported to be involved in a variety of physiological processes, including glucose and lipid metabolism, insulin resistance, and anti-inflammatory effect[9]. Among them, the PPARβ/δ subtype is considered to be an important pharmacological target for the treatment of diabetes and its related diseases in many studies. For example, PPARβ/δ deficient mice exhibit obesity and glucose intolerance under a high-fat diet[10]. PPARβ/δ can also become a promising treatment for patients with diabetes nephropathy through its downstream signal transduction[11].

Current therapies for T2DM involve regulating hormones[12,13] and utilizing bioactive substances from natural plants. For instance, cyanidin-3-O-glucoside (C3G), an anthocyanin in berries, reduces body weight and improves metabolic homeostasis in mice by altering hepatic FGF21[14]. In addition, research has demonstrated that C3G can prevent diabetic nephropathy in rats through the regulation of relevant hormones in vivo[15].

[1]Department of Environmental Health, Zhejiang Provincial Center for Disease Control and Prevention, Hangzhou, China. [2]Innovation Center for Information, Binjiang Institute of Zhejiang University, Hangzhou, China. [3]Department of Food Science and Nutrition, College of Biosystems Engineering and Food Science, Zhejiang University, Hangzhou, China. ✉e-mail: tupengcheng1@163.com

Fig. 1 | Ingredients of anthocyanin extract from red bayberry and its safe concentrations for STC-1 and NIT-1 cells. A The process of anthocyanin extraction and identification. B UPLC profiles of the anthocyanin extract at 520 nm. C STC-1 cell viability was analyzed by cell viability assay (*n* = 6). D NIT-1 cell viability was analyzed by cell viability assay (*n* = 6). Con: negative control under low glucose; C3G: different concentrations of C3G intervention. Any two groups labeled with different letters (e.g., a, b, or c) on the histogram, indicate statistically significant differences ($p < 0.05$).
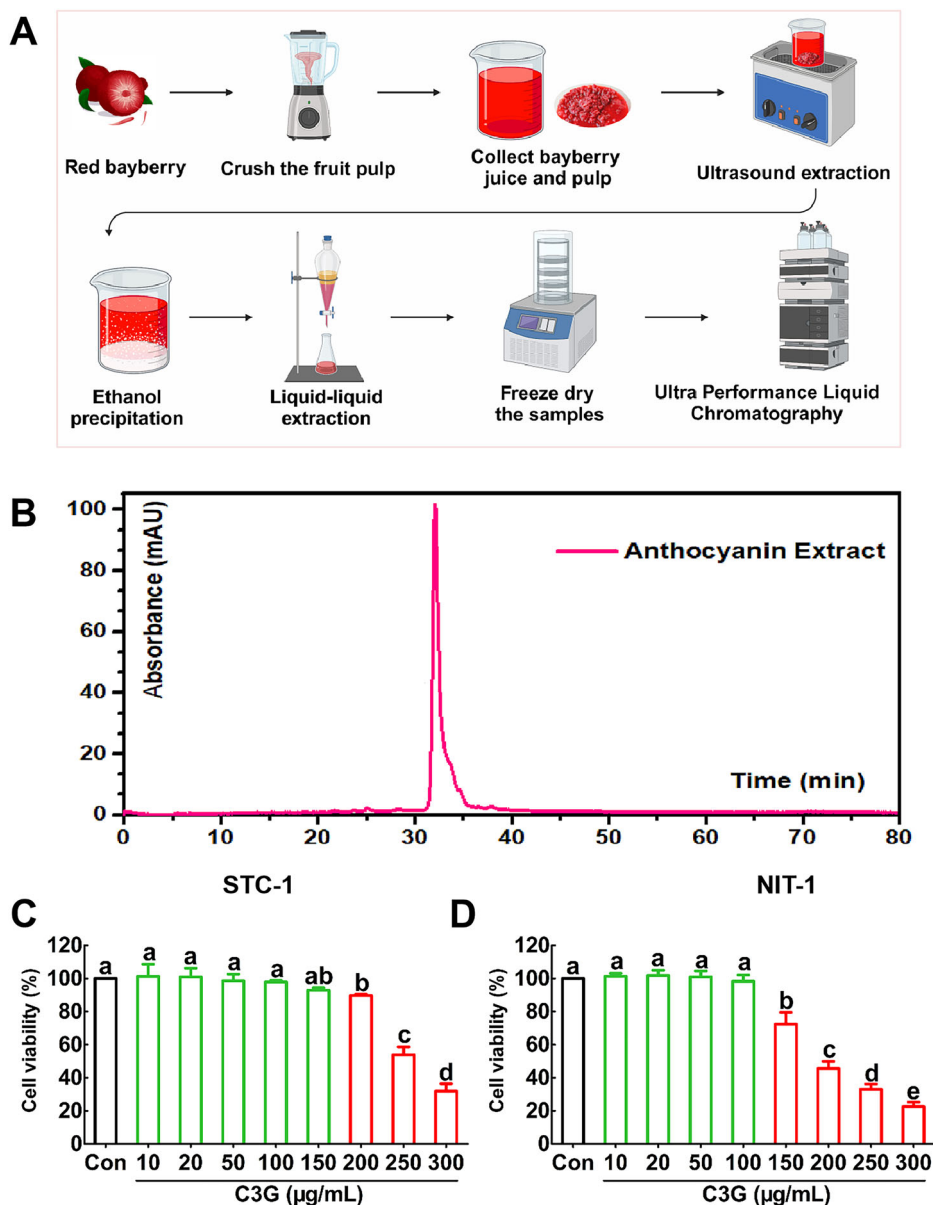
However, there are few studies on whether C3G can ameliorate T2DM by regulating insulin release and its potential mechanisms.

In this work, a cell co-culture system was established to confirm our hypothesis that C3G extracted from red bayberry (*Myrica rubra*) can activate PPARβ/δ expression, enhancing GLP-1 secretion in intestinal L cell STC-1 and consequently increasing insulin release from islet β cell NIT-1.

Results

Ingredients in red bayberry anthocyanin extract and its safe concentrations on STC-1 and NIT-1 cells

The extraction process and ingredient identification of the anthocyanin extract from red bayberry are shown in Fig. 1A. The anthocyanin extract was analyzed using UPLC at a wavelength of 520 nm, and the prominent peak was identified as C3G (Fig. 1B), referring to our previous work[16]. The safe concentration of C3G on STC-1 or NIT-1 cells was assessed using the cell viability assay. Figure 1C shows that incubating STC-1 cells with C3G at concentrations ranging from 10 μg/mL to 150 μg/mL for 24 h did not significantly reduce cell viability. Furthermore, exposure of NIT-1 cells to C3G concentrations between 10 μg/mL and 100 μg/mL for 24 h also did not lead to a significant decrease in cell viability (Fig. 1D). These results indicate that

C3G at concentrations below 100 μg/mL is safe for both STC-1 and NIT-1 cells, and concentrations below 100 μg/mL were selected for further research.

C3G increased insulin levels in NIT-1 cells by stimulating the GLP-1 release from STC-1 cells

In in vitro cell culture, intestinal endocrine L cell line STC-1 can secrete GLP-1, and islet β cell line NIT-1 cells can release insulin. In order to investigate the interaction between intestinal endocrine L cells and islet β cells in the presence of C3G, we established a layered co-culture of STC-1 and NIT-1 cells separated by a transwell insert on a 24-well tissue culture plate (Fig. 2E). The C3G concentrations of 20, 40, and 80 μg/mL were selected based on MTT assay results confirming safety below 100 μg/mL (Fig. 1C, D) and to evaluate dose-dependent effects on GLP-1 secretion and insulin release. As shown in Fig. 2A, B, the concentrations of GLP-1 and insulin in the culture medium were increased in response to the high glucose induction; at the same time, this effect could be significantly enhanced following C3G treatment. To determine the effect of C3G on each cell line, two cell lines were treated separately with C3G. The results indicated that C3G effectively enhanced GLP-1 secretion in STC-1 cells under the high
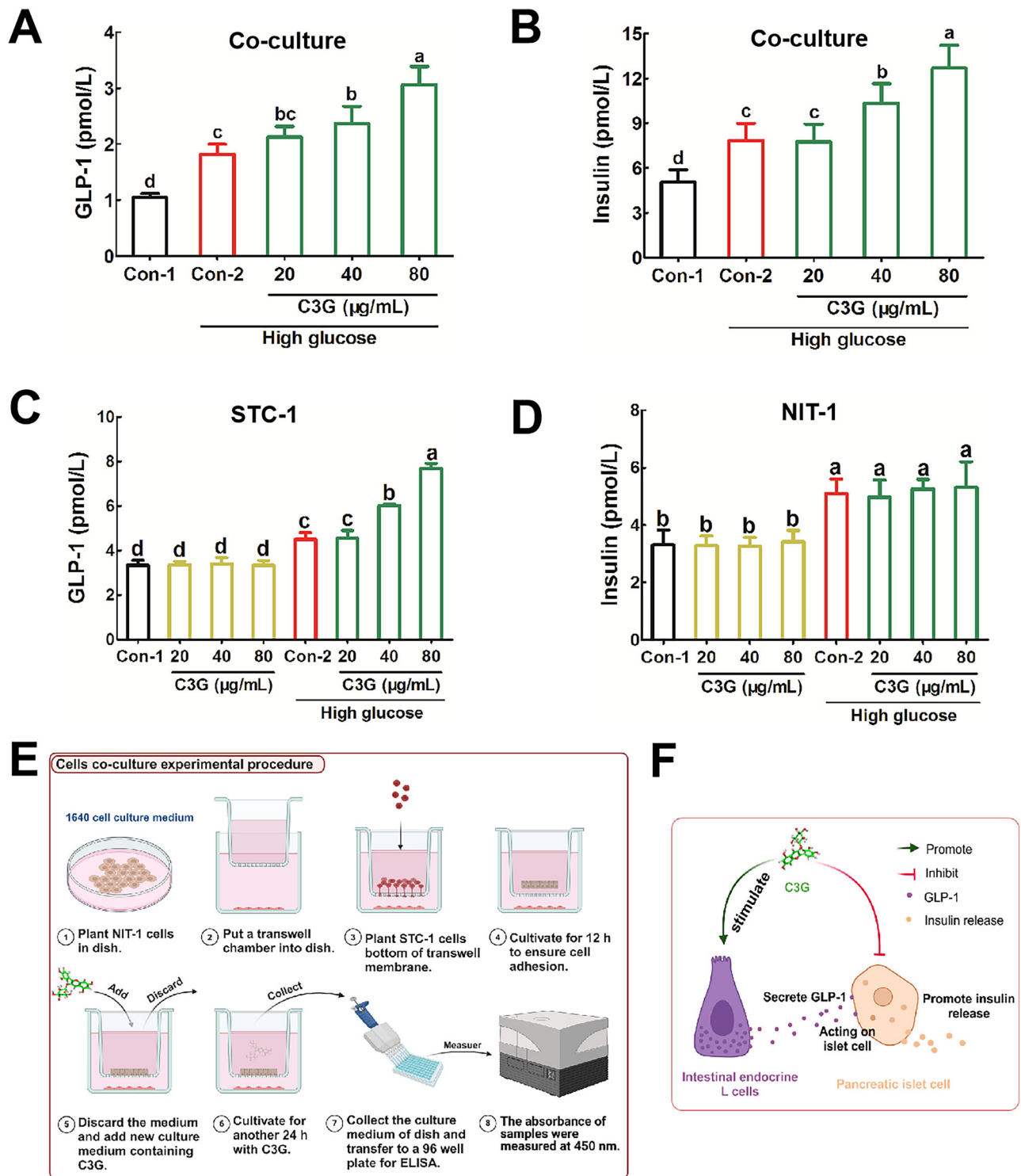
Fig. 2 | C3G stimulated GLP-1 secretion in STC-1 cells to indirectly increase insulin release in NIT-1 cells. A GLP-1 content from culture medium after 24 h STC-1 and NIT-1 co-culture in the presence of C3G ($n = 3$). **B** Insulin content from culture medium after 24 h STC-1 and NIT-1 co-culture in the presence of C3G ($n = 3$). **C** The GLP-1 content from the culture medium after treating STC-1 cells with C3G alone for 24 h ($n = 4$). **D** The insulin content from the culture medium after treating NIT-1 cells with C3G alone for 24 h ($n = 4$). **E** Schematic diagram of steps for cell co-culture. **F** The schematic diagram of C3G stimulates GLP-1 release from STC-1 cells to achieve increased insulin release in NIT-1 cells indirectly. Con-1: negative control under low glucose; Con-2: positive control under high glucose; C3G: 80 µg/mL C3G intervention under high glucose. Any two groups labeled with different letters (e.g., a, b, or c) on the histogram, indicate statistically significant differences ($p < 0.05$).

glucose treatment (Fig. 2C), but C3G did not affect insulin release in NIT-1 cells even under high glucose conditions (Fig. 2D). To further investigate the duration of the effects of C3G on GLP-1 and insulin release, we conducted time course experiments utilizing the optimal concentration of C3G. The

result indicated that GLP-1 secretion and insulin release began to increase within 2 h post-C3G treatment. The effect was sustained and reached its peak at 24 h, after which it gradually declined (Fig. S1). This suggested that the stimulatory effect of C3G on GLP-1 secretion and insulin release is not

Fig. 3 | C3G promoted GLP-1 expression by increasing PG levels in STC-1 cells. A The mRNA expression of PG in STC-1 cells ($n = 3$). **B** The mRNA expression of GLP-1 in STC-1 cells ($n = 3$). **C** Protein bands of PG and GLP-1 were detected by WB analysis ($n = 3$). **D** Quantitative analysis of protein bands for PG ($n = 3$). **E** Quantitative analysis of protein bands for GLP-1 ($n = 3$). **F** The relationship among C3G, PG, and GLP-1. Con-1: negative control under low glucose; Con-2: positive control under high glucose; C3G: 80 μg/mL C3G intervention under high glucose. Any two groups labeled with different letters (e.g., a, b, or c) on the histogram, indicate statistically significant differences ($p < 0.05$).
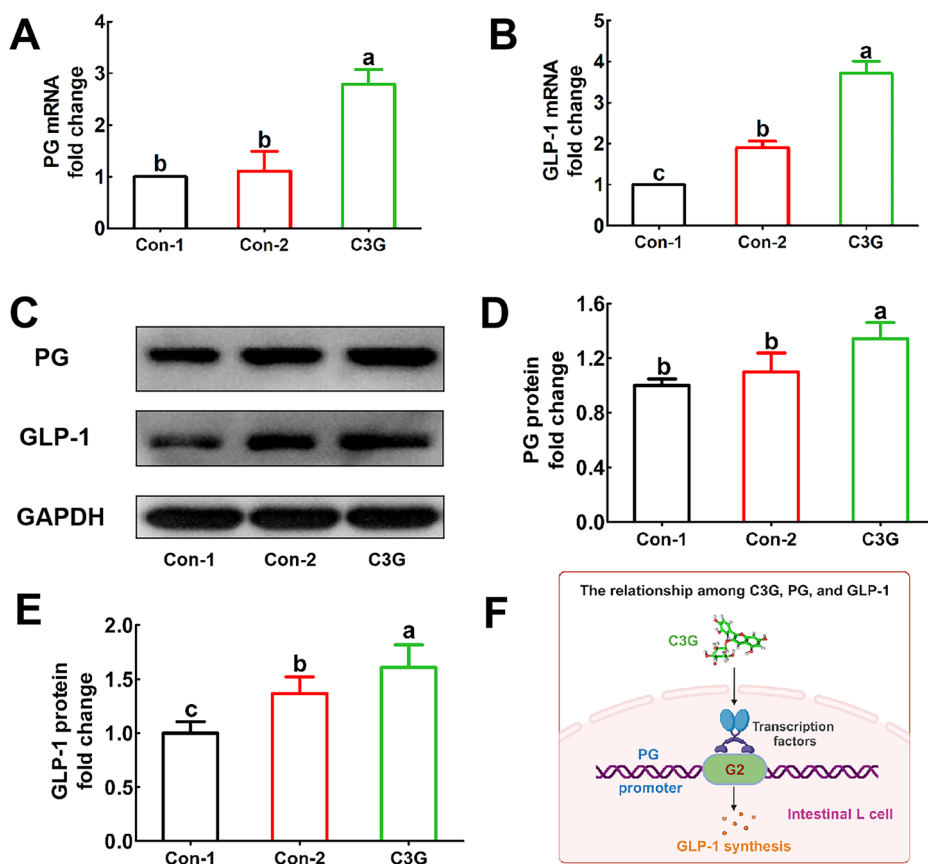
only acute but also persistent, lasting up to 24 h. Accordingly, a treatment duration of 24 h was selected for the subsequent experiments. These findings suggested that the increased insulin release associated with C3G treatment, primarily results from C3G stimulating intestinal endocrine L cell STC-1 to secrete GLP-1 rather than directly affecting islet β cell NIT-1 in a high glucose environment (Fig. 2F).

C3G increased the expression of PG to enhance GLP-1 expression in high glucose-induced STC-1 cells

The intracellular expression of PG, a key precursor of GLP-1, is a critical determinant of GLP-1 secretion from intestinal L cells, as previously established in the literature[17]. Our data indicated that the transcription of PG and GLP-1 is enhanced upon incubation with C3G under high glucose stimulation, as evidenced by increased mRNA levels of PG (Fig. 3A) and GLP-1 (Fig. 3B) in STC-1 cells. Furthermore, under the same treatment conditions, WB analysis was conducted to measure the protein expressions of PG and GLP-1. As shown in Fig. 3C–E, the protein expression levels of both PG and GLP-1 were elevated in response to C3G treatment in STC-1 cells. These findings collectively suggested that C3G exerts its regulatory effect on GLP-1 secretion by upregulating PG expression, thereby providing a mechanistic basis for its role in modulating GLP-1 release from intestinal L cells (Fig. 3F).

C3G activated the PPARβ/δ-β-catenin-TCF-4 pathway in STC-1 cells

Previous studies have established the critical role of the PPARβ/δ signaling pathway in intracellular PG synthesis[18]. In this study, as shown in Fig. 4A-E, GW501516, a PPARβ/δ agonist, significantly upregulated protein expression in the β-catenin-TCF-4 pathway by activating PPARβ/δ. Similarly, treatment with C3G also increased the protein expression of PPARβ/δ, β-catenin, and TCF-4 in a dose-dependent manner. Notably, while high glucose treatment elevated the protein expression of GLP-1 (Figs. 3C, E), it

did not affect the protein expressions of PPARβ/δ and its downstream target genes (Fig. 4B–E). These findings demonstrate that C3G activates PPARβ/δ, thereby stimulating the β-catenin-TCF-4 pathway (Fig. 4F).

C3G upregulated PG in STC-1 cells by activating the PPARβ/δ-β-catenin-TCF-4 pathway to promote GLP-1 expression

To further investigate the role of the PPARβ/δ-β-catenin-TCF-4 pathway in C3G-induced upregulation of PG and GLP-1 expression in intestinal endocrine L cells, we employed GSK0660, a specific inhibitor of PPARβ/δ. STC-1 cells were pre-treated with GSK0660 for 2 h, followed by the incubation of C3G for another 24 h. As shown in Fig. 5A–F, activation of the PPARβ/δ-β-catenin-TCF-4 pathway by C3G upregulated PG expression and enhanced high glucose-induced GLP-1 expression in STC-1 cells. However, C3G-induced GLP-1 protein expression was inhibited in conjunction with decreased expressions of PPARβ/δ, β-catenin, and TCF-4 following GSK0660 treatment. Moreover, the effects of C3G on insulin metabolism during co-culture, including GLP-1 secretion (Fig. 5G) and insulin release (Fig. 5H), was also blocked in the presence of GSK0660. In contrast, high glucose-induced GLP-1 release was unaffected by PPARβ/δ inhibition, suggesting that C3G-induced PG gene transcription to increase GLP-1 levels in STC-1 cells was specifically mediated through the PPARβ/δ-β-catenin-TCF signaling pathway.

Discussion

In our present study, two cell lines were selected as the research models, namely STC-1 cell derived from the mouse intestine, which is the gut endocrine cell that secretes GLP-1 and is currently recognized as the best cell line for studying GLP-1 secretion[19]. In contrast, the NIT-1 cell, a islet β cell line, mainly releases insulin under glucose stimulation, making it an ideal model for studying glucose metabolism and insulin secretion. Utilizing these two cell lines, the in vitro co-culture system was established within a transwell chamber, which allowed the two layers of cells to interact with each
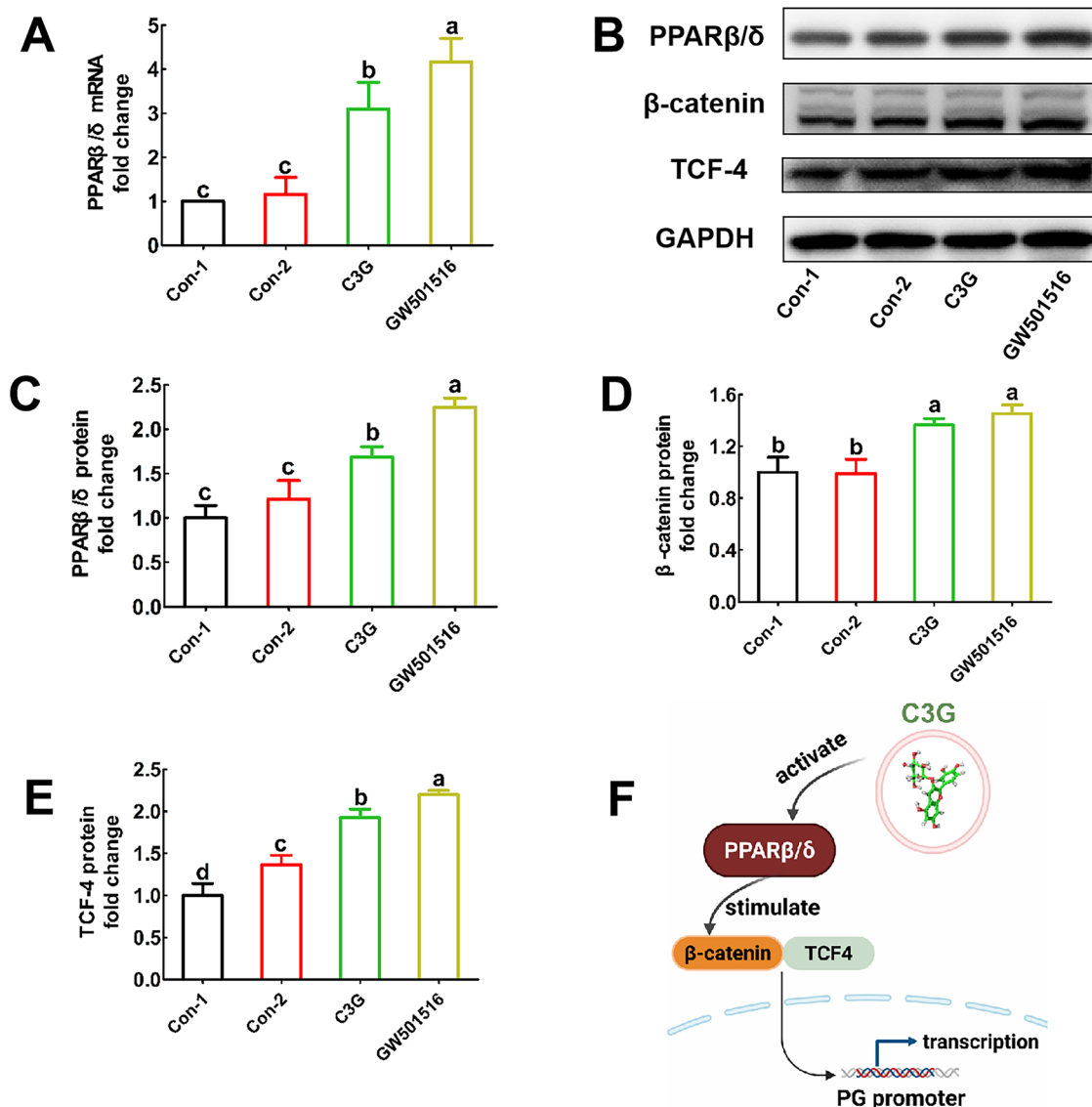
Fig. 4 | C3G activated the PPARβ/δ-β-catenin-TCF-4 signaling pathway in STC-1 cells. A The mRNA expression of PPARβ/δ ($n = 3$). **B** Protein bands of PPARβ/δ, β-catenin, and TCF-4 were detected by WB ($n = 3$). **C** Quantitative analysis of protein bands for PPARβ/δ ($n = 3$). **D** Quantitative analysis of protein bands for β-catenin ($n = 3$). **E** Quantitative analysis of protein bands for TCF-4 ($n = 3$). **F** The role of the PPARβ/δ-β-catenin-TCF-4 pathway in the regulation of C3G on PG transcription. Con-1: negative control under low glucose; Con-2: positive control under high glucose; C3G: 80 μg/mL C3G intervention with high glucose; GW501561: PPARβ/δ agonist GW501516 intervention under high glucose. Any two groups labeled with different letters (e.g., a, b, or c) on the histogram, indicate statistically significant differences ($p < 0.05$).

other, to investigate the interactions between C3G, GLP-1 secretion, and insulin release.

Our results indicated an increase in the levels of GLP-1 and insulin in the culture medium after 24 h co-culture with C3G, particularly under high glucose conditions. However, when C3G was administered to STC-1 cells or NIT-1 cells separately, the NIT-1 cells were unable to release insulin under either low or high glucose conditions. On the contrary, C3G significantly enhanced GLP-1 secretion from STC-1 cells under high glucose conditions. These findings highlight a key distinction in the effects of C3G on these two cell types. Specifically, C3G directly stimulates GLP-1 secretion from STC-1 cells, its effect on insulin release from NIT-1 cells appears to be mediated indirectly. These suggest that C3G may initiate a cascade of cellular responses that enhance glucose-dependent insulin release, likely through the paracrine action of GLP-1 secreted from STC-1 cells.

The observed increase in GLP-1 and insulin levels following C3G treatment raises essential questions about the underlying mechanisms.

GLP-1 is a vital incretin hormone that plays a significant role in glucose metabolism and insulin secretion. Otherwise, PG is a precursor substance for GLP-1, which is enzymatically cleaved to GLP-1 by prohormone convertase 1 in intestinal L cells[20]. Therefore, monitoring alterations in PG expression within intestinal L cells is essential for understanding GLP-1 secretion. Our results indicate that C3G treatment significantly increased PG and GLP-1 protein expressions, thereby promoting GLP-1 release through PG regulation.

The next issue we explored concerns the transcription factors involved in C3G modulates PG and GLP-1 expression. Prior study has reported that the activation of PPARβ/δ, a nuclear receptor involved in pancreatic islet function and glucose homeostasis, promotes GLP-1 secretion by intestinal L cells. Researchers also showed that the GW501516 is a kind of PPARβ/δ agonist and could stimulate the β-catenin-TCF-4 signaling pathway in cells[21]. Given that the PG promoter is a potential target of the β-catenin-TCF-4 pathway[18], it is
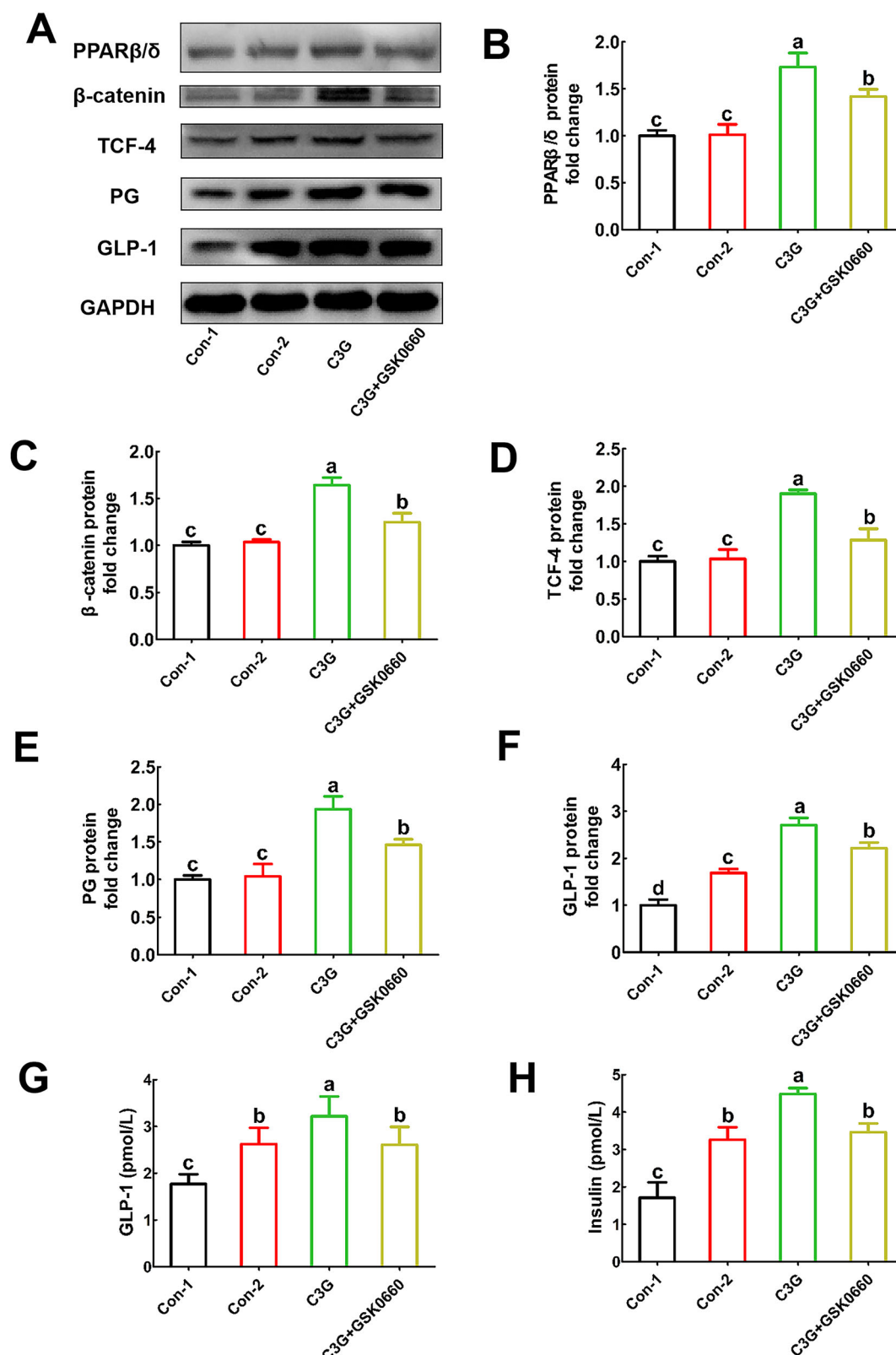
Fig. 5 | The regulation of C3G on GLP-1 secretion in STC-1 cells was achieved through the activation of the PPARβ/δ-β-catenin-TCF-4 signaling pathway. A Protein bands of PPARβ/δ, β-catenin, TCF-4, PG, and GLP-1 were detected by WB ($n = 3$). B Quantitative analysis of protein bands for PPARβ/δ ($n = 3$). C Quantitative analysis of protein bands for β-catenin ($n = 3$). D Quantitative analysis of protein bands for TCF-4. E Quantitative analysis of protein bands for PG ($n = 3$). F Quantitative analysis of protein bands for GLP-1 ($n = 3$). G GLP-1 content from the culture medium ($n = 3$). H Insulin content from the culture medium ($n = 3$). Con-1: negative control under low glucose; Con-2: positive control under high glucose; C3G: 80 μg/mL C3G intervention with high glucose; C3G + GSK0660: Co intervention of 80 μg/mL C3G and PPARβ/δ inhibitor GSK0660 under high glucose. Any two groups labeled with different letters (e.g., a, b, or c) on the histogram, indicate statistically significant differences ($p < 0.05$).

reasonable to infer that PPARβ/δ may regulate PG by activating this pathway. In this study, we first demonstrated that PPARβ/δ agonist GW501516 can stimulate the PPARβ/δ-β-catenin-TCF-4 signaling pathway in STC-1 cells. Moreover, building on Jia's findings that PPARβ/δ is a potential target of C3G[22], and our results show that C3G mirrors GW501516 in activating PPARβ/δ-β-catenin/TCF-4 signaling pathway. We provide evidence that C3G potentially activated the PPARβ/δ-β-catenin/TCF-4 signaling pathway to promote PG transcription and GLP-1 secretion. Beyond its role in enhancing GLP-1 secretion through the regulation of PG, this pathway has been implicated in various other metabolic processes. For instance, the PPARβ/δ-β-catenin-TCF-4 pathway has been shown to regulate metabolic homeostasis by modulating the expression of FGF21, which is involved in glucose and lipid metabolism[14]. Additionally, this pathway may influence inflammation by modulating inflammatory factors, potentially reducing metabolic inflammation in conditions such as obesity and T2DM[9]. Furthermore, PPARβ/δ has been linked to the regulation of lipid metabolism genes, promoting lipid oxidation and fatty acid metabolism[10]. Finally, the pathway has been associated with promoting islet β cell proliferation and function, which is critical for maintaining glucose homeostasis[12]. These findings highlight the multifaceted role of the PPARβ/δ-β-catenin-TCF-4 pathway in metabolic regulation and underscore its potential as a therapeutic target for T2DM. A summary of these downstream targets and their functions is provided in Table S2.

A PPARβ/δ inhibitor, GSK0600, was employed at a concentration of 0.2 μM to validate the critical role of the PPARβ/δ-β-catenin-TCF-4 pathway in mediating GLP-1 release in response to C3G treatment. This concentration was chosen based on previous studies demonstrating that 0.2 μM GSK0660 is sufficient to inhibit PPARβ/δ activity in both cellular and animal models[23]. Our data showed that the upregulation of PG and GLP-1 expression induced by C3G was significantly attenuated in the presence of a PPARβ/δ inhibitor. The inhibition of this pathway by GSK0600 underscored its essential role in mediating the effects of C3G. The marked reduction of PG and GLP-1 expressions in the presence of PPARβ/δ inhibitors confirms that the action of C3G is not merely a broad stimulation of cellular function but rather a targeted modulation of specific signaling pathways that govern hormone secretion. Consistent findings in the co-culture system further corroborated these observations. Our investigation into the signaling pathways revealed that the activation of the PPARβ/δ-β-catenin-TCF-4 pathway is a crucial driver of the C3G-induced enhancement of GLP-1 secretion.

While our study provides valuable insights into the mechanisms by which C3G enhances GLP-1 secretion and insulin release, several limitations should be acknowledged. Firstly, our research was primarily conducted using in vitro models, which may not fully recapitulate the complex physiological environment in vivo. Future studies should validate these findings in animal models and further evaluate the long-term effects of C3G therapy on glucose homeostasis and insulin sensitivity, as well as the potential side effects of long-term use of C3G. Secondly, the concentrations of C3G used in our experiments may not directly translate to achievable levels through dietary intake alone, suggesting that supplementation strategies may need to be considered. Thirdly, while C3G is a natural flavonoid compound found in various fruits and vegetables and is generally considered safe for consumption as part of a regular diet, excessive intake or long-term use at high doses may pose unknown risks. Future research, particularly long-term animal experiments, is needed to fully understand the safety profile of C3G when used as a supplement over extended periods. Finally, our study focused on the role of the PPARβ/δ-β-catenin-TCF-4 pathway, but other potential pathways and interactions may also play a role and warrant further investigation.

Our study reveals that C3G indirectly increases insulin release from islet NIT-1 cells by stimulating intestinal STC-1 cells to secrete GLP-1. This effect is achieved through the activation of the PPARβ/δ-β-catenin-TCF-4 signaling pathway within intestinal L cells, suggesting its potential in T2DM management. As a natural flavonoid in fruits and vegetables, C3G

offers a cost-effective, orally available option to complement GLP-1 receptor agonists, with particular benefits for resource-limited settings. It may also synergize with existing therapies to amplify GLP-1 signaling and reduce medication dosages, while preserving islet β cell function in high-risk individuals. Future research should focus on optimizing the dose, bioavailability, and long-term effects of C3G, and exploring its interaction with gut microbiota to pave the way for novel dietary or pharmacological strategies enhancing metabolic health in T2DM.

Methods
Materials and reagents
The intestinal L cell line STC-1 and islet cell line NIT-1 were obtained from the Chinese Academy of Sciences. The enzyme-linked immunosorbent assay (ELISA) kits were purchased from Jingmei Biotechnology (Jiangsu, China). Primary antibodies against GAPDH (2118-T, 1:10000 dilution) and PG (D16G10, 1:1000 dilution) were obtained from Cell Signaling Technology (Shanghai, China). Primary antibodies against GLP-1 (AG1995, 1:1000 dilution), PPARβ/δ (AF7800, 1:2000 dilution), TCF-4 (AF8106, 1:2000 dilution), and β-catenin (AF5126, 1:500 dilution), as well as secondary antibodies (goat anti-mouse and anti-rabbit, 1:1000 dilution), were obtained from Beyotime Biotechnology (Shanghai, China). Reagents for western blotting (WB), enhanced chemiluminescence (ECL) kit, and BCA protein assay kit were sourced from Beyotime Biotechnology (Shanghai, China). Other chemical reagents were purchased from Aladdin (Shanghai, China).

Preparation and identification of red bayberry anthocyanin
According to the extraction method established by our team[24], red bayberry (*Myrica rubra*) fruit pulp was extracted with four volumes of anhydrous ethanol using ultrasonication for 1.5 h. This extraction was repeated three times. The filtered solution was evaporated at 49 °C and centrifuged. The supernatant was collected and mixed with ethyl acetate in a 1:1 volume ratio for liquid-liquid extraction. The aqueous phase was collected until the organic phase was clarified, and then the aqueous phase was evaporated at 49 °C to remove residual organic solvents. The collected liquid sample was loaded onto a D101 macroporous resin column and sequentially eluted with 1% formic acid in 80% methanol for further purification. Finally, the purified red bayberry anthocyanin was identified using a Promosil C18 column (4.6 × 250 mm, 5 μm) on an Ultra Performance Liquid Chromatography (UPLC) system (Thermo Ultimate 3000).

Cell culture and treatments
The intestinal endocrine L cell line STC-1 and islet cell line NIT-1 were cultured in RPMI 1640 medium supplemented with 5 mM glucose, 10% fetal bovine serum, 100 U/mL penicillin, and 100 μg/mL streptomycin in 100 mm cell culture dishes at 37 °C in a 5% CO_2 atmosphere.

To establish stratified co-culture of STC-1 and NIT-1 cells in 24-well plates using transwell, STC-1 cells were first plated on top of the matrigel and then NIT-1 cells were cultured in 24-well plates. Once cells reached 75–85% confluence, they were treated with different concentrations of C3G (20, 40, and 80 μg/mL) for 24 h.

Cell viability assay
3-(4, 5-Dimethylthiazol-2-yl)-2, 5-diphenyltetrazolium bromide (MTT), diluted in PBS to 0.5 mg/mL, was added to a 96-well plate at 100 μL per well, where STC-1 or NIT-1 cells were cultured. The plate was incubated at 37 °C in a 5% CO_2 atmosphere for 3–4 hours. Following the incubation, 150 μL of dimethyl sulfoxide was added to each well to dissolve the formazan precipitate. The absorbance was measured at 570 nm using a microplate reader to determine the cell viability.

ELISA analysis
After standing at room temperature for 20 min, 50 μL of the diluted sample was added to each well of GLP-1 or insulin antibody-coated 96-well plate. Subsequently, 50 μL of peroxidase-coupled secondary antibody was

distributed to each well and incubated for 1 h at 37 °C. The plate was then washed five times with a wash buffer. Following this, 100 μL of mixed substrate was added to each well for the revelation reaction, which was performed in the dark for 15 min. Afterward, 50 μL of stop solution was added and mixed for 30 s to terminate the reaction. Finally, the absorbance of each sample was measured at 450 nm using a microplate reader.

RNA isolation, reverse transcription, and qRT-PCR analysis

Total RNA from STC-1 cells was extracted using an RNA miniprep kit (Takara, 9108). RNA was then reverse-transcribed into cDNA using an RT reagent kit (Takara, RR047A). qRT-PCR was performed on an Applied Biosystems Step One System (Thermo Fisher Scientific) using the TB Green kit (Takara, RR420A). Primer sequences for target genes are listed in Table S1.

WB analysis

Protein extracts from treated cells were prepared using WB/IP lysis buffer. The protein extracts were separated by 12% SDS-polyacrylamide gel electrophoresis and then electroblotted onto polyvinylidene difluoride membranes. The blotted membranes were blocked with blocking solution at 25 °C for 60 min, followed by overnight incubation at 4 °C with primary antibodies against PG, GLP-1, PPARβ/δ, β-catenin, TCF-4, and GAPDH. Membranes were washed three times with PBST to remove residual primary antibodies and then incubated with horseradish peroxidase-conjugated goat anti-rabbit or goat anti-mouse IgG secondary antibodies at 25 °C for 60 min. Following secondary antibody incubation, blotted membranes were washed three times with PBST to remove residual secondary antibodies. Finally, protein bands were detected using an ECL detection reagent and visualized using a digital imaging system.

Statistical analyses

Data are expressed as means ± SD. Statistical analyses were performed using SPSS 16.0 software. Fluorescence image intensity was quantified using Image-Pro Plus 6.0 software. WB protein band intensity was quantified using Image J software. All the experimental results are based on three or more independent replicate experiments. Any two groups labeled with different letters (e.g., a, b, or c) on the histogram, indicate statistically significant differences ($p < 0.05$).

Data availability

No datasets were generated or analyzed during the current study.

References

1. Lernmark B., Hansson G., Larsson H., Lindberg B., Sjöblad S. Does genetic screening for Type 1 diabetes in newborns affect mothers and fathers in the same way? Acad. Green Energy (2003).
2. Groop, L. C., Widén, E. & Ferrannini, E. Insulin resistance and insulin deficiency in the pathogenesis of Type 2 (non-insulin-dependent) diabetes mellitus : errors of metabolism or of methods. *Diabetologia* **36**, 1326–1331 (1993).
3. Novak, U., Wilks, A., Buell, G. & Mcewen, S. Identical mRNA for preproglucagon in pancreas and gut. *Eur. J. Biochem.* **164**, 553–558 (1987).
4. Scrocchi, L. A., Marshall, B. A., Cook, S. M., Brubaker, P. L. & Drucker, D. J. Identification of glucagon-like peptide 1 (GLP-1) actions essential for glucose homeostasis in mice with disruption of GLP-1 receptor signaling. *Diabetes* **47**, 632–639 (1998).
5. Toft-Nielsen, M. et al. Determinants of the impaired secretion of glucagon-like peptide-1 in type 2 diabetic patients. *J. Clin. Endocrinol. Metab.* **86**, 3717–3723 (2001).
6. Klonoff, D. C. et al. Exenatide effects on diabetes, obesity, cardiovascular risk factors and hepatic biomarkers in patients with type 2 diabetes treated for at least 3 years. *Curr. Med. Res. Opin.* **24**, 275–286 (2008).
7. Holst J. J. Glucagon and glucagon-like peptides 1 and 2. In: Rehfeld J.F., Bundgaard J.R. (eds.) 221–234 (Springer Berlin Heidelberg; 2010).
8. Ni, Z. et al. Transcriptional activation of the proglucagon gene by lithium and β-catenin in intestinal endocrine L cells. *J. Biol. Chem.* **278**, 1380–1387 (2003).
9. Christofides, A., Konstantinidou, E., Jani, C. & Boussiotis, V. A. The role of peroxisome proliferator-activated receptors (PPAR) in immune responses. *Metab. Clin. Exp.* **114**, 154338 (2021).
10. Lee, C. H. et al. PPARdelta regulates glucose metabolism and insulin sensitivity. *Proc. Natl. Acad. Sci.USA* **103**, 3444–3449 (2006).
11. Chang, J. T., Liang, Y. J. & Leu, J. G. Glucagon-like peptide-1 receptor regulates receptor of advanced glycation end products in high glucose-treated rat mesangial cells. *J. Chin. Med. Assoc.* **86**, 39–46 (2023).
12. Chon, S. & Gautier, J. F. An update on the effect of incretin-based therapies on β-cell function and mass. *Diabetes Metab. J.* **40**, 99–114 (2016).
13. Andersen, A., Lund, A. & Knop, F. K. Vilsbøll T. Glucagon-like peptide 1 in health and disease. *Nat. Rev. Endocrinol.* **14**, 390–403 (2018).
14. Tian, L. et al. Dietary cyanidin-3-glucoside attenuates high-fat-diet–induced body-weight gain and impairment of glucose tolerance in mice via effects on the hepatic hormone FGF21. *J. Nutr.* **150**, 2101–2111 (2020).
15. Qi, S. S. et al. Cyanidin-3-glucoside from black rice prevents renal dysfunction and renal fibrosis in streptozotocin-diabetic rats. *J. Funct Foods* **72**, 104062 (2020).
16. Ye, X. et al. Food-derived cyanidin-3- O -glucoside alleviates oxidative stress: evidence from the islet cell line and diabetic db/db mice. *Food Funct.* **12**, 11599–11610 (2021).
17. Taşçı, S. K. & Bingöl, S. A. GLP-1 localisation and proglucagon gene expression in healthy and diabetic mouse ileum. *J. Vet. Res.* **62**, 237–242 (2018).
18. Daoudi, M. et al. PPARβ/δ activation induces enteroendocrine L cell GLP-1 production: PPARβ/δ activation increases gut GLP-1 production. *Gastroenterology* **140**, 1564–1574 (2011).
19. Thomas, C. et al. TGR5-mediated bile acid sensing controls glucose homeostasis. *Cell Metab.* **10**, 167–177 (2009).
20. Whalley, N. M., Pritchard, L. E., Smith, D. M. & White, A. Processing of proglucagon to GLP-1 in pancreatic α-cells: is this a paracrine mechanism enabling GLP-1 to act on β-cells? *J. Endocrinol.* **211**, 99 (2011).
21. Han, C., Lim, K., Xu, L., Li, G. & Wu, T. Regulation of Wnt/beta-catenin pathway by cPLA2alpha and PPARdelta. *J. Cell Biochem.* **105**, 534–545 (2008).
22. Jia, Y. et al. Cyanidin is an agonistic ligand for peroxisome proliferator-activated receptor-alpha reducing hepatic lipid. *Biochim. Biophys. Acta* **1831**, 698–708 (2013).
23. Antonosante, A. et al. Neuroprotective effects of the PPARβ/δ antagonist GSK0660 in in vitro and in vivo Parkinson's disease models. *Biol. Res.* **56**, 27 (2023).
24. Chen, W., Zheng, X., Yan, F., Xu, L. & Ye, X. Modulation of gut microbial metabolism by cyanidin-3-O-glucoside in mitigating polystyrene-induced colonic inflammation: insights from 16S rRNA sequencing and metabolomics. *J. Agric. Food Chem.* **72**, 7140–7154 (2024).

Acknowledgements

Author contributions

Xiang Ye: Writing - Original Draft, Validation, Formal analysis, Visualization, Methodology, Data Curation, Investigation. Wen Chen: Formal analysis, Visualization, Methodology, Investigation. Fujie Yan: Resources, Funding acquisition. Xiaodong Zheng: Methodology, Resources, Supervision. Pengcheng Tu: Methodology, Writing - Review & Editing, Funding acquisition, Resources, Project administration, Supervision.

Competing interests

The authors declare no competing interests.

Additional information

Supplementary information The online version contains supplementary material available at https://doi.org/10.1038/s41538-025-00445-4.

Correspondence and requests for materials should be addressed to Pengcheng Tu.

Reprints and permissions information is available at http://www.nature.com/reprints

Publisher's note Springer Nature remains neutral with regard to jurisdictional claims in published maps and institutional affiliations.